

1 Development, characterization and application of an improved online 2 reactive oxygen species analyzer based on MARGA

3 Jiyao Wu^{1,2}, Chi Yang^{1,2}, Chunyan Zhang^{1,2}, Fang Cao^{1,2}, Aiping Wu^{1,2}, Yanlin Zhang^{1,2}

4 *

5 ¹ Yale-NUIST Center on Atmospheric Environ., Joint International Research
6 Laboratory of Climate and Environment Change (ILCEC), Nanjing University of
7 Information Science and Technology, Nanjing 210044, China

8 ² School of Applied Meteorology, Nanjing University of Information Science and
9 Technology, Nanjing 210044, China

10 Correspondence: Yanlin Zhang (zhangyanlin@nuist.edu.cn)

11 Abstract

12 Excessive reactive oxygen species (ROS) in the human body is an important factor
13 leading to diseases. Therefore, research on the content of reactive oxygen species in
14 atmospheric particles is necessary. In recent years, the online detection technology of
15 ROS has been developed. However, there are few technical studies on online detection
16 of ROS based on the DTT method. Here, to modify the instrument, it is added a DTT
17 experimental module that is protected from light and filled with nitrogen at the end,
18 based on the Monitor for AeRosols and Gases in ambient Air (MARGA). The
19 experimental study found that the detection limit of the modified instrument is 0.024
20 nmol min⁻¹. The DTT consumption rate of blank sample (ultra-pure water) is reduced
21 by 44 %, which eliminates the influence of outside air and light in the experiment. And
22 the accuracy of the online instrument is determined by comparing the online and offline
23 levels of the samples, which yielded good consistency (slope 0.97, R²=0.95). It shows
24 that the performance of the instrument is indeed optimized, the instrument is stable, and
25 the characterization of ROS is accurate. The instrument not only realizes the online
26 detection conveniently and quickly, but also achieves the hour-by-hour detection of
27 ROS based on the DTT method. Meanwhile, reactive oxygen and inorganic ions in
28 atmospheric particles are quantified using the online technique in the northern suburbs
29 of Nanjing. It is found that the content of ROS during the day is higher than that at night,
30 especially after it rains, ROS peaks appear in the two time periods of 08:00-10:00 and
31 16:00-18:00. In addition, examination of the online ROS and water-soluble ions (SO₄²⁻,
32 NO₃⁻, NH₄⁺, Na⁺, Ca²⁺, K⁺), BC and polluting gases (SO₂, CO, O₃, NO, NO_x)
33 measurements revealed that photo-oxidation and secondary formation processes could
34 be important sources of aerosol ROS. This method breakthrough enables the
35 quantitative assessment of atmospheric particulate matter ROS at the diurnal scale,
36 providing an effective tool to study sources and environmental impacts of ROS.

37 1、 Introduction

38 Air quality is a major issue affecting human health, and prolonged exposure to
39 high ambient particulate concentrations can lead to a significant increase in the
40 probability of respiratory and cardiovascular diseases, which can seriously impair
41 human health (Delfino et al., 2005; Ghio et al., 2012; Pöschl and Shiraiwa, 2015). The
42

43 production of reactive oxygen species (ROS) in the human body is the most reliable
44 pathophysiological mechanism proposed, and excessive reactive oxygen species can
45 cause an imbalance between the oxidative system and the antioxidant system, causing
46 oxidative stress and tissue damage (Ahmad et al., 2021; Akhtar et al., 2010; Borm et al.,
47 2007; Delfino et al., 2013; Lodovici and Bigagli, 2011). Thus, oxidative potential (OP)
48 has been proposed as a more biologically relevant indicator than particulate matter (PM)
49 mass concentration to represent the combined effects of multiple toxic components in
50 PM (Ayres et al., 2008; Hellack et al., 2015; Janssen et al., 2015). Understanding the
51 generation mechanism and source characteristics of reactive oxygen species is essential
52 for making reasonable pollution control decisions and reducing their impact on human
53 health.

54 In recent years, the analysis method of oxidation potential has cell detection and
55 cell-free detection. To provide a simpler and quicker way to determine the oxidation
56 potential of environmental particulate matter, cell-free methods such as electron spin
57 (or paramagnetic) resonance (OP_{ESR}), dithiothreitol assay (OP_{DTT}), ascorbic acid assay
58 (OP_{AA}), high-performance liquid chromatography (HPLC) and glutathione assay
59 (OP_{GSH}) are often used as the main measurement methods for ROS (Bates et al., 2019;
60 Ghio et al., 2012). Through the comparison and analysis of these various methods by a
61 large number of researchers, the DTT method is generally considered to be the most
62 common and comprehensive method to reflect the magnitude of the chemical oxidation
63 potential of particulate matter (Hedayat et al., 2014; Xiong et al., 2017).

64 Generally, the cell-free method still has problems with detection delays and
65 degradation of particulate chemical components during sample storage, which not only
66 leads to inaccurate detection data, but also the inability to capture daily changes.
67 Therefore, the development of online detection technology becomes necessary
68 (Charrier et al., 2016; Dou et al., 2015; Fang et al., 2017; Li et al., 2012; Liu et al., 2014;
69 Velali et al., 2016; Vreeland et al., 2017). So far, the development of online detection
70 technology is mainly based on the DCFH method and the DTT method. On the one
71 hand, an online detection technology based on the DCFH method has been reported
72 previously (Eiguren-Fernandez et al., 2017; Huang et al., 2016; Sameenoi et al., 2012;
73 Wragg et al., 2016). However, some researchers believe that in the DCFH method, the
74 horseradish peroxidase (HRP) will promote the production of hydroxyl free radicals,
75 leading to an overestimation of ROS content (Pal et al., 2012). On the other hand, based
76 on the DTT method to develop online detection technology (Fang et al., 2014;
77 Puthussery et al., 2018), The semi-automatic detection system researched by Fang et al,
78 based on the DTT method cannot realize an online collection of environmental samples.
79 On this basis, Puthussery et al used a mist chamber (MC) to continuously collect $PM_{2.5}$
80 in environmental water and realized fully automatic hourly ROS detection.

81 However, these detection methods ignore the influence of air and light on the
82 experiment. As the main reagent of the experiment, dithiothreitol (DTT) and 5,5'-
83 dithiobis (2-nitrobenzoic acid) (DTNB) are easily oxidized by air (Chen et al., 2010).
84 We achieve accurate measurement of the oxidation potential of environmental
85 particulates by shielding from light and filling with nitrogen. In addition, the present
86 study is developed on the basis of the MARGA, which is a state-of-art instrument.

87 MARGA measures near-real-time water-soluble particulate species and their gaseous
88 precursors (Chen et al., 2017). MARGA is used to collect particulate matter and is
89 connected to the optimized DTT_v detection part to observe the oxidation potential hour
90 by hour. The system realizes simultaneous observation of oxidation potential and
91 inorganic ions. Here, we optimize the performance of the instrument and measure the
92 hourly averaged OP of ambient PM_{2.5}. The reliability of online detection of oxidation
93 potential data is supported by analyzing the correlation between ions, polluting gases,
94 BC and oxidation potential.

95 **2、 Materials and Method**

96 **2.1 Instrument set-up and improvement**

97 Figure 1 shows the scheme and schematic diagram of the system for DTT online
98 detection. The instrument is set up in the Atmospheric Environ. monitoring laboratory
99 on the roof of the Wende Building of Nanjing University of Information Engineering
100 (30 m above the ground) and the room temperature is maintained at 20°C. The entire
101 system is composed of the MARGA, the automatic sample-receiving device, and the
102 DTT experimental reaction device. The MARGA is used as an instrument for detecting
103 atmospheric aerosols and inorganic components of gases (water-soluble ions Cl⁻、NO₃⁻、
104 SO₄²⁻、NH₄⁺、Na⁺、K⁺、Mg²⁺、Ca²⁺), and it collects gases using a wet rotary separator
105 and aerosols using steam injection, and absorbs gases and aerosols into the aqueous
106 phase separately to separate them from each other. Then, the resulting solution is
107 analyzed by ion chromatography equipped with a conductivity detector. That is, the gas
108 and aerosol are analyzed separately to detect the gas precursors and different ionic
109 compositions in the aerosol.

110 In past studies, MARGA was often used to detect the content of inorganic
111 components of atmospheric aerosols and gases in cities around the world (Rumsey et
112 al., 2014). And Chen et al. conducted a special evaluation study on the accuracy and
113 precision of MARGA (Chen et al., 2017). In addition, Stieger et al. achieved
114 quantitative analysis of low molecular weight organic acids in the atmospheric gas
115 phase and particle phase by modifying MARGA (Stieger et al., 2019). Hemmilä et al
116 used a MARGA ligation an electrospray ionization quadrupole mass spectrometer (MS)
117 to achieve 1-hour resolution quantification of 7 different amines in gas and particulate
118 phases in forest air in northern Finland. (Hemmilä et al., 2018) As a mature commercial
119 instrument, MARGA can measure the inorganic components of atmospheric aerosols
120 and gases with 1-hour resolution. In this study, based on MARGA, the DTT
121 experimental part is connected to realize the hour-by-hour simultaneous detection of
122 aerosol inorganic components and ROS.

123 In the DTT reaction module, to avoid the influence of light and air on the
124 experiment, all pipelines, reaction flasks and mixing flasks are sealed and protected
125 from light by aluminum foil. The whole DTT experimental part was filled with N₂ by
126 pump A and pump B before the experiment started. In addition, we added a refrigerator
127 to store DTT, DTNB and other experimental solutions. During the DTT experiment, the
128 reaction tube and mixing tube were placed in an incubator at 37°C to simulate the
129 temperature of human lungs. To realize the subsequent DTT experimental reactions, as

130 in Figure 1 we collected the liquid-phase aerosols into sample tubes through a dual-
131 channel split-flow controlled-volume peristaltic pump. And set peristaltic pump 1 speed
132 to 1.55 ml h⁻¹ to finish 1.5 ml h⁻¹ sample volume.

133 Finally, the determination of DTT activity is achieved by the continuous regular
134 operation of the programmable pumps A and B and the detection of the
135 spectrophotometer. (see Sect. 2.2.1 for details)

136 **2.2 Method**

137 **2.2.1 Online DTT assay measurement**

138 The whole measurement step is divided into three steps: sample collection, DTT
139 reaction part, and spectrophotometer detection. In the first step (the sample collection),
140 the MARGA will discharge 25 ml of aerosol liquid every hour, and use the dual-channel
141 split flow control volume peristaltic pump 1 to add 1.55 ml of the solution (to ensure
142 1.5 ml of sample) into the sample tube, and the rest will enter the automatic sampling
143 device to save through the peristaltic pump 2 (the automatic sampler is set to rotate one
144 grid per hour).

145 In the second step (the part is protected from light and in a nitrogen environment),
146 the reaction part is divided into a DTT oxidation step and a DTT determination
147 step(Wang et al., 2019). First (DTT oxidation step), use pump A to add 5 mL potassium
148 phosphate buffer (0.1 mol L⁻¹), 1.5 mL aerosol extract sample, and 0.5 mL DTT (1
149 mmol L⁻¹) into the mixing bottle (MV) in sequence. Inhale ultrapure water to clean the
150 syringe of pump A. DTT reacts with the aerosol extract in MV. To adapt to the
151 experimental process, the concentration and addition volume of each substance are
152 changed in the experiment, but the concentration of each substance in the mixed
153 solution is similar to that of Cho et al. (Cho et al., 2005). Lin et al. found that the initial
154 DTT concentration will affect the final DTT_v value (Lin et al., 2019). During the
155 experiment, the initial DTT concentration was always kept at 1 mM, so it did not affect
156 the judgment of the daily change of ROS content.

157 Second (DTT determination step), after completing the first step, at 0.10.20.30.40
158 minutes, use pump A to draw 1ml mixed solution in the mixing bottle and add it to the
159 reaction bottle. Then, immediately add 1 mL TCA (10% w/v; quencher) to the reaction
160 vial (RV, wrapped in aluminum foil to prevent possible light interference) using pump
161 A. Add 0.05 mL DTNB (1 mmol L⁻¹) via pump B and mix. The residual DTT reacts
162 with DTNB to form light absorption product 2-nitro-5-thiobenzoic acid (TNB) with
163 high extinction performance at 412 nm.

164 In the third step, in the detection part of the spectrophotometer, use pump A to add
165 4 mL Tris buffer (0.4 mol L⁻¹, containing 20 mmol L⁻¹ EDTA) into the reaction flask
166 (RV). After the reaction is completed, use pump A to add the final mixture solution in
167 the reaction flask to the LWCC for the absorbance test. The data acquisition software
168 (Spectra Suite) records the absorbance at 412 and 700 nm every 10 min (select the
169 baseline absorbance of TNB). Then, the system uses deionized water (deionized water)
170 for self-cleaning to eliminate any residual liquid in the reaction flask, tubing, syringe,
171 and LWCC. To determine the rate of DTT consumption, the time interval is 10 min, and
172 a total of 6 (0 min, 10 min, 20 min, 30 min, 40 min, 50 min) data points of DTT

173 concentration over time are generated. Finally, the automated system performs the self-
174 cleaning procedure again to ensure that there is no residue, and the system repeats the
175 above operations in the next hour to realize hourly detection of DTT activity.

$$176 \quad \Delta DTT = -\sigma Abs \cdot \frac{N_0}{Abs_0} \quad (1)$$

$$177 \quad DTT_v = \frac{\Delta DTT_s(\text{nmol min}^{-1}) - \Delta DTT_b(\text{nmol min}^{-1})}{V_t(\text{m}^3) \times \frac{V_s(\text{mL})}{V_e(\text{mL})}} \quad (2)$$

178 where σAbs is the slope of absorbance versus time; Abs_0 is the initial absorbance
179 calculated from the intercept of the linear regression of absorbance versus time; and N_0
180 is the initial moles of DTT added in the reaction vial. $\Delta DTT_s(\text{nmol min}^{-1})$ is the DTT_v
181 consumption rate of the sample, $\Delta DTT_b(\text{nmol min}^{-1})$ is the blank DTT consumption
182 rate, $V_t(\text{m}^3)$ is the sampling volume corresponding to the sample, and $V_s(\text{mL})$ is the
183 injection volume, $V_e(\text{mL})$ is the sampling volume.

184 **2.2.2 Online DTT instrument performance**

185 The performance of the automated system is characterized by testing to determine
186 the instrument response, limit of detection (LOD), precision and accuracy, while using
187 a large flow sampler to collect samples for offline and online comparative analysis. (See
188 Sect.3.1 for details)

189 We perform DTT activity detection and comparison on samples collected by 9,10-
190 phenanthraquinone (PQN) and offline high-flow samplers. First, we select PQN with
191 concentrations of 0.01, 0.02, 0.025, 0.05, 0.085 nmol L⁻¹ to compare online and offline
192 DTT activity detection to determine the error of online and offline experiments. The
193 details of PQN analysis can be found in Supplement S1. Secondly, select 10 offline
194 collected samples for online and offline comparison, and then combine the
195 experimental error between online and offline determined by PQN (PQN online and
196 offline orthogonal fitting) to analyze the accuracy of online and offline.

197 **2.2.3 Instrument maintenance**

198 The MARGA is calibrated using internal and external standards. The internal
199 standard is a 10 mg L⁻¹LiBr solution. The external standard calibration is performed
200 after replacing the anion and cation columns, and the replacement cycle is generally 4
201 to 5 months. At the same time, the MARGA system is cleaned with 1% hydrogen
202 peroxide and 10% acetone solution, and the airflow is calibrated every two months. In
203 the DTT experimental module, DTT and DTNB solutions are prepared every 4 days.
204 Before each test, perform a comprehensive light and nitrogen bag inspection. To ensure
205 the accuracy of the experimental data, a standard curve was measured before each
206 experiment. The instrument pipeline is cleaned once a week, as shown in Figure 1. The
207 programmable pump A and pump B are connected to the ultrapure water channel.
208 During the cleaning process, all pipelines, reaction tubes and mixing tubes are cleaned.

209 **2.3 Collection and preparation of environmental samples**

210 The sampling point is located on the roof of the seventh floor of the Maintenance
211 Branch (34°58' N, 117°26' E) of the Power Company, Yunlong District, Xuzhou City.
212 The surrounding buildings mainly include auto repair shops, logistics centers,
213 pharmaceutical factories, and large residential areas and farmland. A large flow PM_{2.5}

214 sampler (KC-6120) is used for continuous sampling, and a total of 10 samples are
215 collected (October 21, 2018-October 31, 2018). When sampling, the flow rate is 1.0 m^3
216 min^{-1} , and each sampling time is 24 h. In this study, we collected samples using quartz
217 filters and stored them in a refrigerator at $-26 \text{ }^\circ\text{C}$. Before the start of the experiment, the
218 collected samples were subjected to extraction processing, and a sample film with a
219 diameter of 16 mm is cut into a brown glass bottle, 5 ml ultrapure water is added to
220 shake for 30 min, and filtered with a $0.22 \text{ }\mu\text{m}$ PTFE syringe filter to remove insoluble
221 substances.

222 **3. Results and discussion**

223 **3.1 Instrument performance**

224 **3.1.1 Improvement of the instrument**

225 As we all know, photo-oxidation promotes the generation of ROS (Fang et al.,
226 2016; Visentin et al., 2016; Yang et al., 2014). In addition, during the measurement
227 process, the ingress of air inside the instrument will also cause the DTT activity to
228 increase. Therefore, before on-site deployment, the online DTT inspection instrument
229 is optimized by filling in nitrogen gas and shielding the whole from light. And
230 respectively detect the DTT consumption rate (ΔDTT) of 10 blanks (ultra-pure water)
231 before and after optimization. As shown in Figure 3, before the system optimization,
232 we found that the average ΔDTT measured by 10 blanks was $0.25\pm 0.04 \text{ nmol min}^{-1}$,
233 and there is a big fluctuation. After optimization, the average ΔDTT is $0.14\pm 0.008 \text{ nmol}$
234 min^{-1} . It shows that air and light do promote the generation of ROS, and the nitrogen
235 environment and avoiding light contribute to the stability of the system. The optimized
236 system is more accurate in measuring the oxidation potential of environmental
237 particulate matter. To further prove the optimization effect, the performance of the
238 instrument is studied. (See Sect.3.1.4 for details)

239 **3.1.2 Calibration of DTT_v measurement and analysis system**

240 In past studies, PQN is often used as a standard sample of atmospheric particulate
241 matter (Charrier and Anastasio, 2011; Charrier and Anastasio, 2015; Xiong et al., 2017).
242 At pH 7.0, almost 100% of DTT was transformed to DTT-Disulfide by the catalyst 9,10-
243 PQ (Li et al., 2009). The analytical measurement part of the online DTT instrument is
244 calibrated by measuring the DTT activity of PQN at different concentrations. As shown
245 in Figure 4, the linear graph of DTT consumption rate and PQN concentration, which
246 is after subtracting the blank DTT consumption rate. The online detection slope is
247 3.66 ± 0.26 , and the coefficient $R^2=0.992$. During the on-site operation, PQN's online
248 and offline testing is measured at least once a month to ensure online accuracy.

249 **3.1.3 Limit of detection and precision**

250 The limit of detection (LOD) of the system is defined as 3 times the standard
251 deviation of the deionized water blank ($N = 23$), i.e., $0.024 \text{ nmol min}^{-1}$, which is
252 significantly lower than the LOD of Puthussery et al. ($0.24 \text{ nmol min}^{-1}$) and Fang et al.
253 ($0.31 \text{ nmol}\cdot\text{min}^{-1}$) (Fang et al., 2014; Puthussery et al., 2018). To ensure the accuracy
254 of the system, the deionized water blank samples are taken once a day (14 days) during
255 the sampling period, besides the 10 continuously measured during the optimization of
256 the system.

257 Use deionized water to evaluate the accuracy of the environmental sample
258 automation system and analyze the DTT activity. The low standard deviation
259 (coefficient of variation, CV=5.61%) of 0.024 nmol min⁻¹ indicates that the system has
260 sufficiently high accuracy for environmental samples.

261 **3.1.4 Accuracy**

262 The accuracy of the system is verified by comparing the DTT activity of the
263 positive control and environmental particulate samples obtained from the automated
264 method with the results obtained from the same experimental protocol performed
265 manually. (Cho et al., 2005)

266 Five concentrations of PQN solutions (0.01, 0.02, 0.025, 0.05, 0.085 nmol L⁻¹) are
267 run in the automatic system, which is very close to the results of the manual system (the
268 standard deviation of the automatic system is kept at 0.008 nmol min⁻¹, and the
269 coefficient of variation is 2.28 %; the standard of the manual system The difference is
270 0.0044 nmol min⁻¹, the coefficient of variation is 1.48 %). As shown in Figure 5, the
271 slope (manual/automatic) obtained by orthogonal fitting is 1.14, the intercept is 0.12,
272 and the correlation coefficient (R²) is 0.997. The manual detection results are slightly
273 higher than the automatic detection results, we assume that this is due to the instrument
274 error caused by the complicated piping system of the online instrument. To ensure the
275 high accuracy of the online system and the offline system, as a further verification, we
276 used online and offline manual methods to conduct DTT activity analysis on ten
277 environmental particulate matter samples.

278 As shown in Figure 6, the online and offline analysis of the DTT activity of 10
279 ambient particles, the slope (manual/automatic) obtained by orthogonal fitting is 1.14,
280 the intercept is 0.19, and the correlation coefficient (R²) is 0.954. We found that the real
281 samples tested also had slightly higher offline results than online results. This is similar
282 to our assumption. Therefore, we use the PQN online and offline DTT consumption
283 rate orthogonal fitting result as the system to correct the error, as shown in Figure 6,
284 through the offline and online orthogonal fitting of 10 environmental particulate matter
285 samples before and after the error correction. We found that the corrected results are
286 better (the slope is 0.97 closer to 1, the intercept is 0.05 closer to 0, R²=0.954). The
287 good agreement between the two sampling systems indicates that the DTT
288 measurement of environmental samples has high overall accuracy. These tests also
289 proved the necessity of optimization.

290 **3.2 DTT activity of ambient samples**

291 The volume-normalized oxidation potential DTT_v is used as an index of exposure
292 to inhaled air to point out the inherent ability of particles to deplete relevant antioxidants.
293 During the observation period, the daily change of DTT_v in Nanjing is shown in Figure
294 7. The average DTT_v is 0.83±0.38 nmol min⁻¹ m⁻³. Compared with Beijing's DTT_v in
295 the spring of 2012 (urban area: 0.24 nmol min⁻¹ m⁻³)(Liu et al., 2014; Wang et al., 2019).
296 and Zhejiang University's annual DTT_v average of 0.62 nmol min⁻¹ m⁻³(Yu et al., 2019) ,
297 our results are on the high side; And compared with Peking University's 2015 annual
298 DTT_v (12.26±6.82 nmol min⁻¹ m⁻³) (Perrone et al., 2016) and Guangzhou's In the winter
299 of 2017 (DTT_v: 4.67±1.06 nmol min⁻¹ m⁻³) and in the spring of 2018 (DTT_v: 4.45±1.02
300 nmol min⁻¹ m⁻³), our values are low, which may be related to the current season and

301 emission factors. In addition, we found that the rain during the sampling period caused
302 significant changes in the 24-hour DTT_v. To better understand the environmental
303 factors affecting DTT_v, hourly data obtained by running the instrument is composited
304 to obtain a diurnal profile of the DTT activity. As shown in Figure S2, the daily
305 distribution of 24-hour DTT activities during the entire sampling period (a), before rain
306 (b), during rain (c), and after rain (d) are divided. Figure S2(a) represents the hourly
307 change of DTT_v during the entire sample period. We found that the highest value of
308 DTT_v in a day occurs at 11-12 am, and DTT_v is greater during the day than at night,
309 which is similar to the study by Puthussery et al. Before the rain, the average DTT_v was
310 $0.81 \pm 0.17 \text{ nmol min}^{-1} \text{ m}^{-3}$. There is a peak at 10-12 am, but the overall situation is
311 relatively flat, and there is no obvious difference between day and night. And the
312 average value of DTT_v during the rain is $0.55 \pm 0.10 \text{ nmol min}^{-1} \text{ m}^{-3}$, which decreased
313 significantly. There is no doubt that this is caused by rain settling the polluting
314 components of the atmosphere. In contrast, there is significant daily activity in DTT_v
315 following rain, with peaks occurring mainly between 8-10 am and 4-6 pm, and DTT_v
316 is significantly higher during the day than at night, which is similar to the Puthussery
317 study (Puthussery et al., 2018). However, there are no obvious diurnal variation in PM_{2.5}
318 mass concentration. Therefore, the diurnal variation of DTT activity is assumed to be
319 mainly attributed from different emission sources at the site.

320 **3.3 The correlation between PM_{2.5} and polluting gases and ROS activity**

321 To further study, the daily changes of DTT_v and its correlation with various
322 emission sources on site. As shown in Figure 7, we measured the water-soluble ionic
323 components of PM_{2.5} (SO₄²⁻, NO₃⁻, NH₄⁺, Na⁺, Ca²⁺, K⁺), BC, and pollution gas (SO₂,
324 CO, O₃, NH₃) content changes. The average concentration of PM_{2.5} during the sampling
325 period is $9.97 \pm 6.53 \text{ ug m}^{-3}$, the average concentration of PM_{2.5} before rain is 11.13 ± 7.21
326 ug m^{-3} , the average concentration of PM_{2.5} after rain is $7.80 \pm 4.18 \text{ ug m}^{-3}$. The
327 concentration of PM_{2.5} is a significant drop. In addition, as shown in Table 1, there are
328 differences in the correlation between PM_{2.5} and DTT_v before and after rain. Therefore,
329 we suspect that the source of DTT_v is different before and after the rain. BC and the
330 polluting gases SO₂, NO_x, NO₂, CO, Ca²⁺, K⁺, Mg²⁺ are often used as tracers of biomass
331 burning, coal combustion, and dust storms. Compared with the early winter in the
332 northern suburbs of Nanjing (Zhang et al., 2020), the levels of these substances
333 decreased during the sampling period. It is similar to Liu and Zhang et al who concluded
334 that biomass burning, coal combustion, and dust storms were not major sources of
335 pollution in Nanjing during the summer (Guo et al., 2019; Liu et al., 2019; Zhang et al.,
336 2020). In addition, there is no strong correlation between DTT_v and SO₂, NO_x, NO₂,
337 and CO before and after the rain. Therefore, it can be judged that neither biomass
338 burning, coal combustion nor dust is the main source affecting DTT_v. In contrast, we
339 found that there is a significant difference between day and night in O₃ after rain, which
340 is similar to the change of DTT_v, and after rain, DTT_v and O₃ show a strong correlation
341 ($r=0.624$). After it rains, the O₃ content in the air environment increases. Under the
342 action of the sun's ultraviolet rays, the O₃ is photodegraded to form active oxygen
343 components such as OH radicals (Ehhalt and Rohrer, 2000; Rohrer and Berresheim,
344 2006).

345 To further confirm the influence of light on DTT_V, the day and night correlation
346 analysis of substances related to photo-oxidation (NH₄⁺, NO₃⁻, SO₄²⁻) and DTT_V is
347 carried out. As shown in Table S2, we find that NH₄⁺, NO₃⁻, SO₄²⁻ and DTT_V are
348 significantly correlated during the day (r=0.434, r=0.461, r=0.263, P<0.01). As far as
349 we know, there is no evidence in the literature that water-soluble inorganic ions (NH₄⁺,
350 NO₃⁻, SO₄²⁻) have redox activity in an aerobic environment(Calas et al., 2018;
351 Stevanovic et al., 2017). However, their correlation with DTT_V may be due to
352 collinearity with redox-active organic compounds, rather than actual contribution to the
353 oxidation potential of particles. We speculate that the high correlation may be related
354 to the photochemical reactions that occur during the day.

355 **4、 Summary and conclusions**

356 This study proposes and characterizes an improved online active oxygen analyzer.
357 Compared with the previous research, the main improvements(Fang et al., 2014;
358 Puthussery et al., 2018). The optimization analysis is as follows: (1) The experimental
359 environment is processed to isolate the air and avoid light; (2) The sampling method
360 has changed. We use the MARGA online ion analyzer, which is more mature and stable.
361 Compared with before optimization, the standard deviation of the blank was
362 significantly smaller, Thus, the detection limit of the instrument (0.024 nmol min⁻¹)
363 becomes smaller and more stable. The DTT consumption rate is reduced by 44 %,
364 which eliminates the influence of outside air and light in the experiment. And the
365 consistency between online and offline is improved (slope=0.97, R²=0.95), the
366 accuracy of the system is higher.

367 By changing the DTT_V content hour by hour during the sampling period, we found
368 that the DTT activity during the day is higher than that at night, and it is especially
369 obvious after rain, which is mainly related to the increase in UV radiation during the
370 day after rain. In addition, we analyzed the correlation between water-soluble ions
371 (SO₄²⁻, NO₃⁻, NH₄⁺, Na⁺, Ca²⁺, K⁺), BC, pollutant gases (SO₂, CO, O₃, NO, NO_x, NH₃)
372 and DTT_V, and we found that the main source of influence of OP in the Nanjing
373 environment in summer is daytime Secondary photochemical conversion and
374 ultraviolet radiation. In the future, we hope to add more experimental modules to the
375 back-end based on the MARGA sample collection device to realize the diversification
376 of detection compositions. In addition, the system can be combined with other
377 substance detection instruments. It will achieve the daily contribution of various
378 emission sources to the risk associated with OP exposure can be inferred from other
379 species.

380

381 *Data availability.* Data used in this paper can be provided upon request by email to
382 ZYL (dryanlinzhang@outlook.com) .

383 *Author contributions.* WJY designed the instrument, led the sampling campaign,
384 performed the experiments, and wrote the manuscript. YC participated in experimental
385 design and guided the experimental process. ZCY chose the building address and
386 initially built the instrument. CF helped in the filter collection and in conducting the
387 DTT activity experiments. ZYL conceived the idea, organized the manuscript, and
388 supervised the project.

389 *Competing interests.* The authors declare that they have no conflict of interest.

390 *Acknowledgements.* The authors thank funding support from the National Nature
391 Science Foundation of China (Nos. 41977305), the Natural Science Foundation of
392 Jiangsu Province (No. BK20180040), the fund from Jiangsu Innovation &
393 Entrepreneurship Team.

394

395 **References:**

- 396 Ahmad, M., Yu, Q., Chen, J., Cheng, S., Qin, W., and Zhang, Y.: Chemical characteristics, oxidative
397 potential, and sources of PM (2.5) in wintertime in Lahore and Peshawar, Pakistan, *J Environ Sci*
398 (China), 102, 148-158, <https://doi.org/10.1016/j.jes.2020.09.014>, 2021.
- 399 Akhtar, U. S., McWhinney, R. D., Rastogi, N., Abbatt, J. P., Evans, G. J., and Scott, J. A.: Cytotoxic and
400 proinflammatory effects of ambient and source-related particulate matter (PM) in relation to the
401 production of reactive oxygen species (ROS) and cytokine adsorption by particles, *Inhal Toxicol*, 22
402 Suppl 2, 37-47, <https://doi.org/10.3109/08958378.2010.518377>, 2010.
- 403 Ayres, J. G., Borm, P., Cassee, F. R., Castranova, V., Donaldson, K., Ghio, A., Harrison, R. M., Hider, R.,
404 Kelly, F., Kooter, I. M., Marano, F., Maynard, R. L., Mudway, I., Nel, A., Sioutas, C., Smith, S., Baeza-
405 Squiban, A., Cho, A., Duggan, S., and Froines, J.: Evaluating the toxicity of airborne particulate matter
406 and nanoparticles by measuring oxidative stress potential--a workshop report and consensus statement,
407 *Inhal Toxicol*, 20, 75-99, <https://doi.org/10.1080/08958370701665517>, 2008.
- 408 Bates, J. T., Fang, T., Verma, V., Zeng, L., Weber, R. J., Tolbert, P. E., Abrams, J. Y., Sarnat, S. E., Klein,
409 M., Mulholland, J. A., and Russell, A. G.: Review of Acellular Assays of Ambient Particulate Matter
410 Oxidative Potential: Methods and Relationships with Composition, Sources, and Health Effects, *Environ.*
411 *Sci. Technol.*, 53, 4003-4019, <https://doi.org/10.1021/acs.est.8b03430>, 2019.
- 412 Borm, P. J. A., Kelly, F., Künzli, N., Schins, R. P. F., and Donaldson, K.: Oxidant generation by particulate
413 matter: from biologically effective dose to a promising, novel metric, *Occup Environ Med*, 64, 73-74,
414 <https://doi.org/10.1136/oem.2006.029090>, 2007.
- 415 Calas, A., Uzu, G., Kelly, F. J., Houdier, S., Martins, J. M. F., Thomas, F., Molton, F., Charron, A., Dunster,
416 C., Oliete, A., Jacob, V., Besombes, J. L., Chevrier, F., and Jaffrezo, J. L.: Comparison between five
417 acellular oxidative potential measurement assays performed with detailed chemistry on PM10 samples
418 from the city of Chamonix (France), *Atmos. Chem. Phys.*, 18, 7863-7875, [https://doi.org/10.5194/acp-](https://doi.org/10.5194/acp-18-7863-2018)
419 [18-7863-2018](https://doi.org/10.5194/acp-18-7863-2018), 2018.
- 420 Charrier, J. G. and Anastasio, C.: Impacts of Antioxidants on Hydroxyl Radical Production from
421 Individual and Mixed Transition Metals in a Surrogate Lung Fluid, *Atmospheric Environ. (Oxford,*
422 *England : 1994)*, 45, 7555-7562, <https://doi.org/10.1016/j.atmosenv.2010.12.021>, 2011.
- 423 Charrier, J. G. and Anastasio, C.: Rates of Hydroxyl Radical Production from Transition Metals and
424 Quinones in a Surrogate Lung Fluid, *Environ. Sci. Technol.*, 49, 9317-9325,
425 <https://doi.org/10.1021/acs.est.5b01606>, 2015.
- 426 Charrier, J. G., McFall, A. S., Vu, K. K. T., Baroi, J., Olea, C., Hasson, A., and Anastasio, C.: A bias in
427 the “mass-normalized” DTT response – An effect of non-linear concentration-response curves for copper
428 and manganese, *Atmospheric Environ.*, 144, 325-334, <https://doi.org/10.1016/j.atmosenv.2016.08.071>,
429 2016.
- 430 Chen, X., Walker, J. T., and Geron, C.: Chromatography related performance of the Monitor for AeRosols
431 and GAses in ambient air (MARGA): laboratory and field-based evaluation, *Atmos. Meas. Tech.*, 10,
432 3893-3908, [10.5194/amt-10-3893-2017](https://doi.org/10.5194/amt-10-3893-2017), 2017.
- 433 Chen, X., Zhong, Z., Xu, Z., Chen, L., and Wang, Y.: 2',7'-Dichlorodihydrofluorescein as a fluorescent
434 probe for reactive oxygen species measurement: Forty years of application and controversy, *Free Radic*
435 *Res*, 44, 587-604, <https://doi.org/10.3109/10715761003709802>, 2010.
- 436 Cho, A. K., Sioutas, C., Miguel, A. H., Kumagai, Y., Schmitz, D. A., Singh, M., Eiguren-Fernandez, A.,
437 and Froines, J. R.: Redox activity of airborne particulate matter at different sites in the Los Angeles Basin,
438 *Environ. Res.*, 99, 40-47, <https://doi.org/10.1016/j.envres.2005.01.003>, 2005.

439 Delfino, R. J., Sioutas, C., and Malik, S.: Potential role of ultrafine particles in associations between
440 airborne particle mass and cardiovascular health, *Environ. Health Perspect.*, 113, 934-946,
441 <https://doi.org/10.1289/ehp.7938>, 2005.

442 Delfino, R. J., Staimer, N., Tjoa, T., Gillen, D. L., Schauer, J. J., and Shafer, M. M.: Airway inflammation
443 and oxidative potential of air pollutant particles in a pediatric asthma panel, *J Expo Sci Environ
444 Epidemiol*, 23, 466-473, <https://doi.org/10.1038/jes.2013.25>, 2013.

445 Dou, J., Lin, P., Kuang, B.-Y., and Yu, J.: Reactive Oxygen Species Production Mediated by Humic-like
446 Substances in Atmospheric Aerosols: Enhancement Effects by Pyridine, Imidazole, and Their
447 Derivatives, *Environ. Sci. Technol.*, 49, <https://doi.org/10.1021/es5059378>, 2015.

448 Ehhalt, D. H. and Rohrer, F.: Dependence of the OH concentration on solar UV, *J. Geophys. Res.:
449 Atmospheres*, 105, 3565-3571, <https://doi.org/10.1029/1999jd901070>, 2000.

450 Eiguren-Fernandez, A., Kreisberg, N., and Hering, S.: An online monitor of the oxidative capacity of
451 aerosols (o-MOCA), *Atmos Meas Tech*, 10, 633-644, <https://doi.org/10.5194/amt-10-633-2017>, 2017.

452 Fang, T., Guo, H., Zeng, L., Verma, V., Nenes, A., and Weber, R. J.: Highly Acidic Ambient Particles,
453 Soluble Metals, and Oxidative Potential: A Link between Sulfate and Aerosol Toxicity, *Environ. Sci.
454 Technol.*, 51, 2611-2620, <https://doi.org/10.1021/acs.est.6b06151>, 2017.

455 Fang, T., Verma, V., Guo, H., King, L., Edgerton, E., and Weber, R.: A semi-automated system for
456 quantifying the oxidative potential of ambient particles in aqueous extracts using the dithiothreitol (DTT)
457 assay: Results from the Southeastern Center for Air Pollution and Epidemiology (SCAPE), *Atmos Meas
458 Tech Discussions*, 7, 7245-7279, <https://doi.org/10.5194/amtd-7-7245-2014>, 2014.

459 Fang, T., Verma, V., Bates, J., Abrams, J., Strickland, M., Ebel, S., Chang, H., Mulholland, J., Tolbert,
460 P., Russell, A., and Weber, R.: Oxidative potential of ambient water-soluble PM_{2.5} in the
461 southeastern United States: contrasts in sources and health associations between ascorbic acid (AA) and
462 dithiothreitol (DTT) assays, *Atmospheric Chem. Phys.*, 16, <https://doi.org/10.5194/acp-16-3865-2016>,
463 2016.

464 Ghio, A. J., Carraway, M. S., and Madden, M. C.: Composition of air pollution particles and oxidative
465 stress in cells, tissues, and living systems, *J. Toxicol. Environ. Health. Part B, Critical reviews*, 15, 1-21,
466 <https://doi.org/10.1080/10937404.2012.632359>, 2012.

467 Guo, Z., Guo, Q., Chen, S., Zhu, B., Zhang, Y., Yu, J., and Guo, Z.: Study on pollution behavior and
468 sulfate formation during the typical haze event in Nanjing with water soluble inorganic ions and sulfur
469 isotopes, *Atmos Res*, 217, 198-207, <https://doi.org/10.1016/j.atmosres.2018.11.009>, 2019.

470 Hedayat, F., Stevanovic, S., Miljevic, B., Bottle, S., and Ristovski, Z.: Review – Evaluating the molecular
471 assays for measuring the oxidative potential of particulate matter, *Chem Ind Chem Engng*, 21, 31-31,
472 <https://doi.org/10.2298/CICEQ140228031H>, 2014.

473 Hellack, B., Quass, U., Nickel, C., Wick, G., Schins, R. P. F., and Kuhlbusch, T. A. J.: Oxidative potential
474 of particulate matter at a German motorway, *Environ Sci Process Impacts*, 17, 868-876,
475 <https://doi.org/10.1039/c4em00605d>, 2015.

476 Hemmilä, M., Hellén, H., Virkkula, A., Makkonen, U., Praplan, A. P., Kontkanen, J., Ahonen, L.,
477 Kulmala, M., and Hakola, H.: Amines in boreal forest air at SMEAR II station in Finland, *Atmospheric
478 Chem. Phys.*, 18, 6367-6380, 10.5194/acp-18-6367-2018, 2018.

479 Huang, W., Zhang, Y., Zhang, Y., Zeng, L., Dong, H., Huo, P., Fang, D., and Schauer, J. J.: Development
480 of an automated sampling-analysis system for simultaneous measurement of reactive oxygen species
481 (ROS) in gas and particle phases: GAC-ROS, *Atmospheric Environ.*, 134, 18-26,
482 <https://doi.org/10.1016/j.atmosenv.2016.03.038>, 2016.

483 Janssen, N. A., Strak, M., Yang, A., Hellack, B., Kelly, F. J., Kuhlbusch, T. A., Harrison, R. M.,
484 Brunekreef, B., Cassee, F. R., Steenhof, M., and Hoek, G.: Associations between three specific a-cellular
485 measures of the oxidative potential of particulate matter and markers of acute airway and nasal
486 inflammation in healthy volunteers, *Occup Environ Med*, 72, 49-56, [https://doi.org/10.1136/oemed-](https://doi.org/10.1136/oemed-2014-102303)
487 2014-102303, 2015.

488 Li, Q., Wyatt, A., and Kamens, R. M.: Oxidant generation and toxicity enhancement of aged-diesel
489 exhaust, *Atmospheric Environ.*, 43, 1037-1042, [10.1016/j.atmosenv.2008.11.018](https://doi.org/10.1016/j.atmosenv.2008.11.018), 2009.

490 Li, Y., Zhu, T., Zhao, J., and Xu, B.: Interactive enhancements of ascorbic acid and iron in hydroxyl
491 radical generation in quinone redox cycling, *Environ. Sci. Technol.*, 46, 10302-10309,
492 <https://doi.org/10.1021/es301834r>, 2012.

493 Lin, M. and Yu, J. Z.: Dithiothreitol (DTT) concentration effect and its implications on the applicability
494 of DTT assay to evaluate the oxidative potential of atmospheric aerosol samples, *Environ Pollut*, 251,
495 938-944, [10.1016/j.envpol.2019.05.074](https://doi.org/10.1016/j.envpol.2019.05.074), 2019.

496 Liu, Q., Baumgartner, J., Zhang, Y., Liu, Y., Sun, Y., and Zhang, M.: Oxidative potential and
497 inflammatory impacts of source apportioned ambient air pollution in Beijing, *Environ. Sci. Technol.*, 48,
498 12920-12929, [10.1021/es5029876](https://doi.org/10.1021/es5029876), 2014.

499 Liu, X., Zhang, Y. L., Peng, Y., Xu, L., Zhu, C., Cao, F., Zhai, X., Haque, M. M., Yang, C., Chang, Y.,
500 Huang, T., Xu, Z., Bao, M., Zhang, W., Fan, M., and Lee, X.: Chemical and optical properties of
501 carbonaceous aerosols in Nanjing, eastern China: regionally transported biomass burning contribution,
502 *Atmos. Chem. Phys.*, 19, 11213-11233, <https://doi.org/10.5194/acp-19-11213-2019>, 2019.

503 Lodovici, M. and Bigagli, E.: Oxidative stress and air pollution exposure, *J. Toxicol*, 2011, 487074,
504 <https://doi.org/10.1155/2011/487074>, 2011.

505 Pal, A. K., Bello, D., Budhlall, B., Rogers, E., and Milton, D. K.: Screening for Oxidative Stress Elicited
506 by Engineered Nanomaterials: Evaluation of Acellular DCFH Assay, *Dose Response*, 10, 308-330,
507 <https://doi.org/10.2203/dose-response.10-036.Pal>, 2012.

508 Perrone, M. G., Zhou, J., Malandrino, M., Sangiorgi, G., Rizzi, C., Ferrero, L., Dommen, J., and
509 Bolzacchini, E.: PM chemical composition and oxidative potential of the soluble fraction of particles at
510 two sites in the urban area of Milan, Northern Italy, *Atmospheric Environ.*, 128, 104-113,
511 <https://doi.org/10.1016/j.atmosenv.2015.12.040>, 2016.

512 Pöschl, U. and Shiraiwa, M.: Multiphase chemistry at the atmosphere-biosphere interface influencing
513 climate and public health in the anthropocene, *Chemical reviews*, 115, 4440-4475,
514 <https://doi.org/10.1021/cr500487s>, 2015.

515 Puthussery, J. V., Zhang, C., and Verma, V.: Development and field testing of an online instrument for
516 measuring the real-time oxidative potential of ambient particulate matter based on dithiothreitol assay,
517 *Atmos. Meas. Tech.*, 11, 5767-5780, <https://doi.org/10.5194/amt-11-5767-2018>, 2018.

518 Rohrer, F. and Berresheim, H.: Strong correlation between levels of tropospheric hydroxyl radicals and
519 solar ultraviolet radiation, *Nature*, 442, 184-187, <https://doi.org/10.1038/nature04924>, 2006.

520 Sameenoi, Y., Koehler, K., Shapiro, J., Boonsong, K., Sun, Y., Collett, J., Jr., Volckens, J., and Henry, C.
521 S.: Microfluidic electrochemical sensor for on-line monitoring of aerosol oxidative activity, *J. Am. Chem.*
522 *Soc.*, 134, 10562-10568, <https://doi.org/10.1021/ja3031104>, 2012.

523 Stevanovic, S., Vaughan, A., Hedayat, F., Salimi, F., Rahman, M. M., Zare, A., Brown, R. A., Brown, R.
524 J., Wang, H., Zhang, Z., Wang, X., Bottle, S. E., Yang, I. A., and Ristovski, Z. D.: Oxidative potential of
525 gas phase combustion emissions - An underestimated and potentially harmful component of air pollution
526 from combustion processes, *Atmospheric Environ.*, 158, 227-235,

527 <https://doi.org/10.1016/j.atmosenv.2017.03.041>, 2017.

528 Stieger, B., Spindler, G., van Pinxteren, D., Grüner, A., Wallasch, M., and Herrmann, H.: Development
529 of an online-coupled MARGA upgrade for the 2 h interval quantification of low-molecular-
530 weight organic acids in the gas and particle phases, *Atmos. Meas. Tech.*, 12, 281-298,
531 <https://doi.org/10.5194/amt-12-281-2019>, 2019.

532 Velali, E., Papachristou, E., Pantazaki, A., Choli-Papadopoulou, T., Planou, S., Kouras, A., Manoli, E.,
533 Besis, A., Voutsas, D., and Samara, C.: Redox activity and in vitro bioactivity of the water-soluble fraction
534 of urban particulate matter in relation to particle size and chemical composition, *Environ. Pollut.*, 208,
535 774-786, <https://doi.org/10.1016/j.envpol.2015.10.058>, 2016.

536 Visentin, M., Pagnoni, A., Sarti, E., and Pietrogrande, M. C.: Urban PM_{2.5} oxidative potential: Importance
537 of chemical species and comparison of two spectrophotometric cell-free assays, *Environ. Pollut.*, 219,
538 72-79, <https://doi.org/10.1016/j.envpol.2016.09.047>, 2016.

539 Vreeland, H., Weber, R., Bergin, M., Greenwald, R., Golan, R., Russell, A. G., Verma, V., and Sarnat, J.
540 A.: Oxidative potential of PM_{2.5} during Atlanta rush hour: Measurements of in-vehicle dithiothreitol
541 (DTT) activity, *Atmospheric Environ.*, 165, 169-178, <https://doi.org/10.1016/j.atmosenv.2017.06.044>,
542 2017.

543 Wang, J., Lin, X., Lu, L., Wu, Y., Zhang, H., Lv, Q., Liu, W., Zhang, Y., and Zhuang, S.: Temporal
544 variation of oxidative potential of water soluble components of ambient PM_{2.5} measured by dithiothreitol
545 (DTT) assay, *Sci. Total Environ.*, 649, 969-978, <https://doi.org/10.1016/j.scitotenv.2018.08.375>, 2019.

546 Wragg, F. P. H., Fuller, S. J., Freshwater, R., Green, D. C., Kelly, F. J., and Kalberer, M.: An automated
547 online instrument to quantify aerosol-bound reactive oxygen species (ROS) for ambient measurement
548 and health-relevant aerosol studies, *Atmos. Meas. Tech.*, 9, 4891-4900, <https://doi.org/10.5194/amt-9-4891-2016>, 2016.

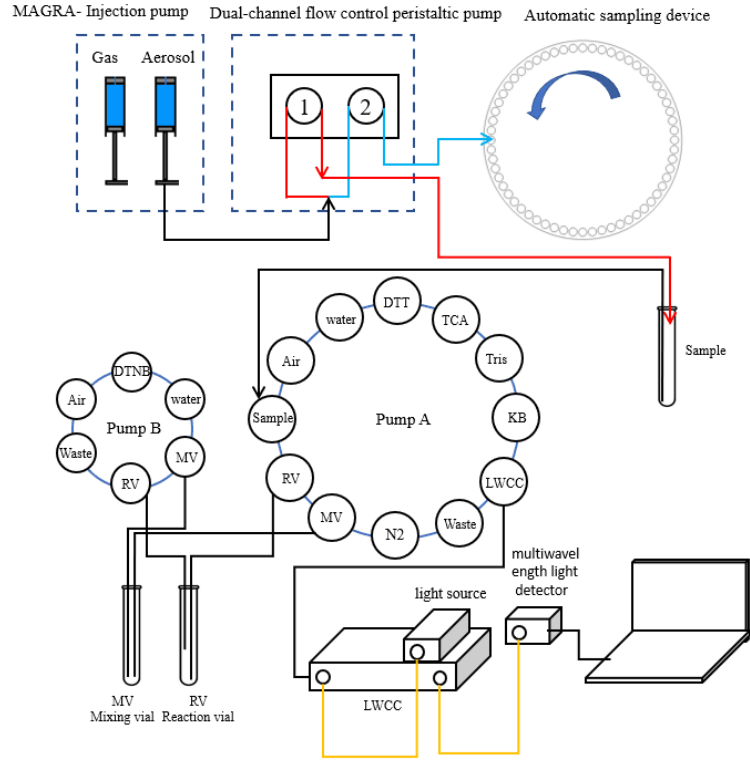
550 Xiong, Q., Yu, H., Wang, R., Wei, J., and Verma, V.: Rethinking Dithiothreitol-Based Particulate Matter
551 Oxidative Potential: Measuring Dithiothreitol Consumption versus Reactive Oxygen Species Generation,
552 *Environ. Sci. Technol.*, 51, 6507-6514, <https://doi.org/10.1021/acs.est.7b01272>, 2017.

553 Yang, A., Jedynska, A., Hellack, B., Kooter, I., Hoek, G., Brunekreef, B., Kuhlbusch, T. A. J., Cassee, F.
554 R., and Janssen, N. A. H.: Measurement of the oxidative potential of PM_{2.5} and its constituents: The effect
555 of extraction solvent and filter type, *Atmospheric Environ.*, 83, 35-42,
556 <https://doi.org/10.1016/j.atmosenv.2013.10.049>, 2014.

557 Yu, S., Liu, W., Xu, Y., Yi, K., Zhou, M., Tao, S., and Liu, W.: Characteristics and oxidative potential of
558 atmospheric PM_{2.5} in Beijing: Source apportionment and seasonal variation, *Sci. Total Environ.*, 650,
559 277-287, <https://doi.org/10.1016/j.scitotenv.2018.09.021>, 2019.

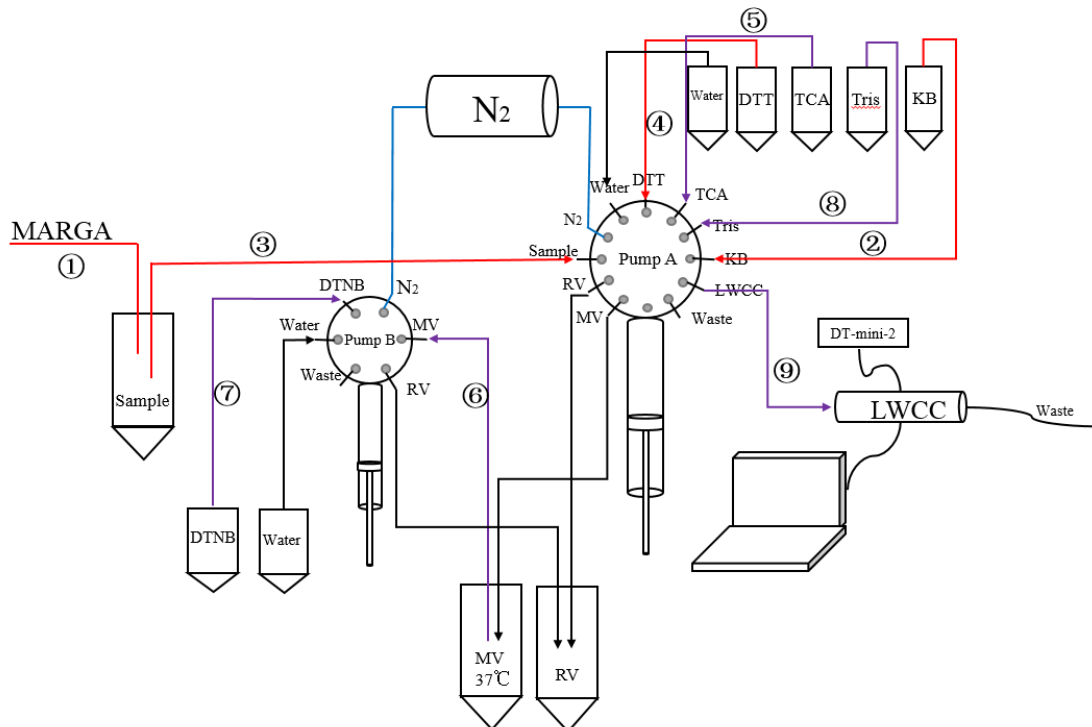
560 Zhang, C., Yang, C., Liu, X., Cao, F., and Zhang, Y.-l.: Insight into the photochemistry of atmospheric
561 oxalate through hourly measurements in the northern suburbs of Nanjing, China, *Sci. Total Environ.*, 719,
562 137416, <https://doi.org/10.1016/j.scitotenv.2020.137416>, 2020.

563



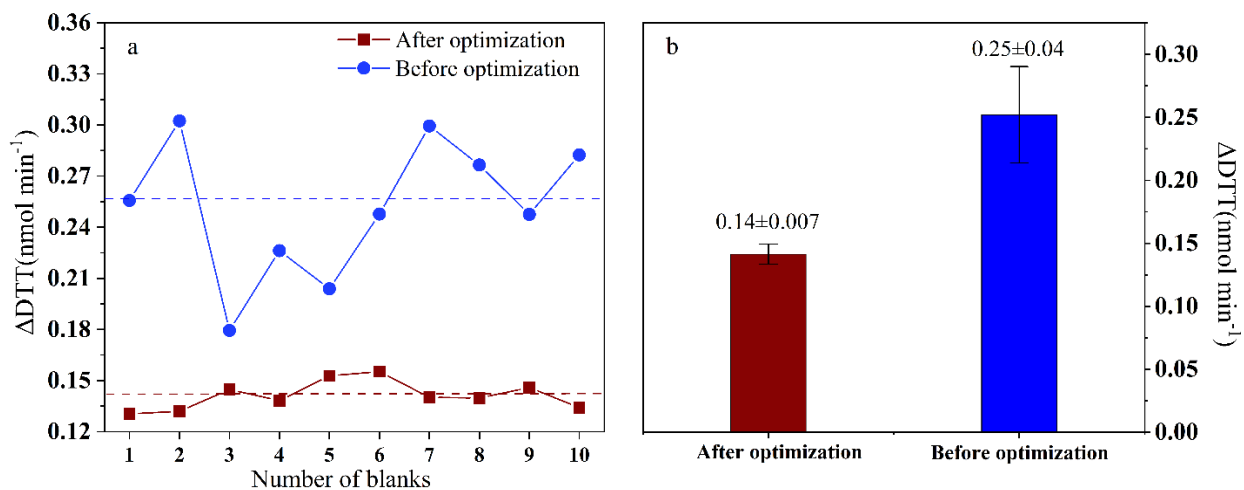
564

565 **Figure 1.** Automated system setup (Red line: Peristaltic pump 1 runs at a flow rate of 23 ml h⁻¹ for the first 4 minutes of each hour; Blue line: Peristaltic pump 2 runs at a flow rate of 27 ml h⁻¹ for the
 566 remaining 56 minutes of each hour; Yellow line: Optical fiber)
 567



568

569 **Figure.2** Schematic diagram of DTT reaction part. (①-④ represents the DTT oxidation step,⑤-⑨
 570 represents the DTT determination step. Blue indicates the ventilation line, all pipelines are wrapped
 571 in aluminum foil to protect from light.)

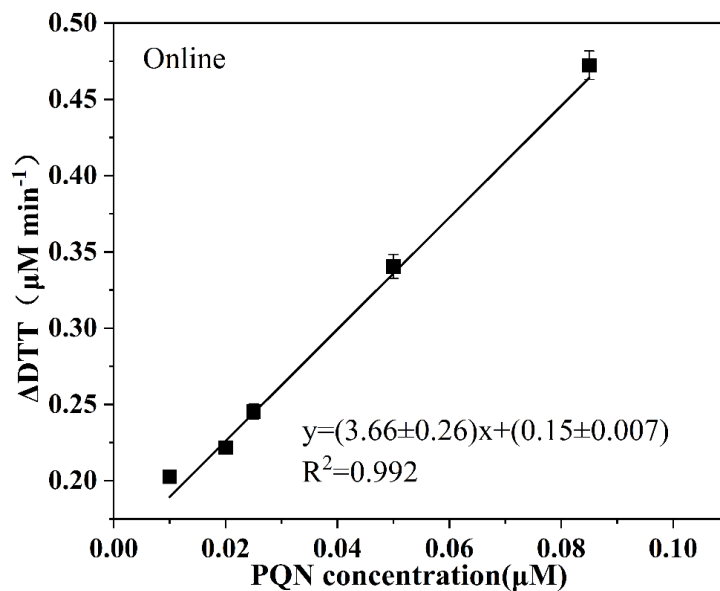


572

573

574

Figure 3. Comparison of blank DTT consumption rate and standard deviation after system optimization (the dotted line is the average value)



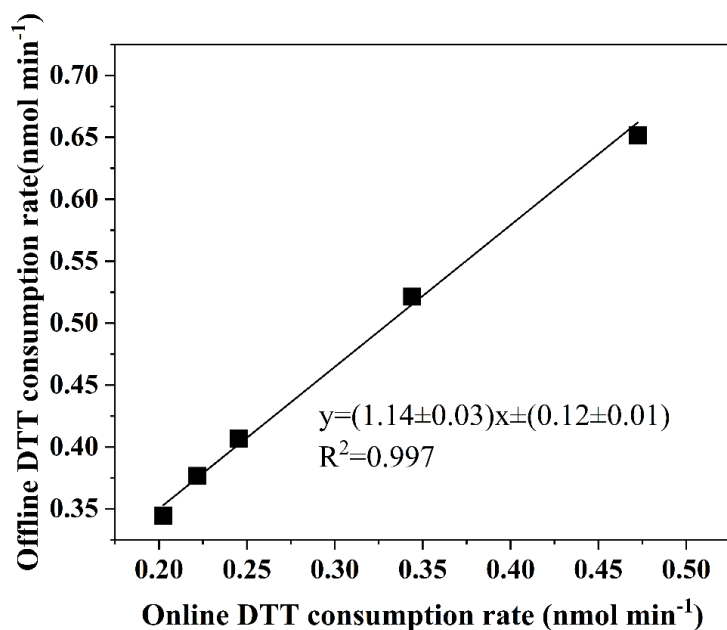
575

576

577

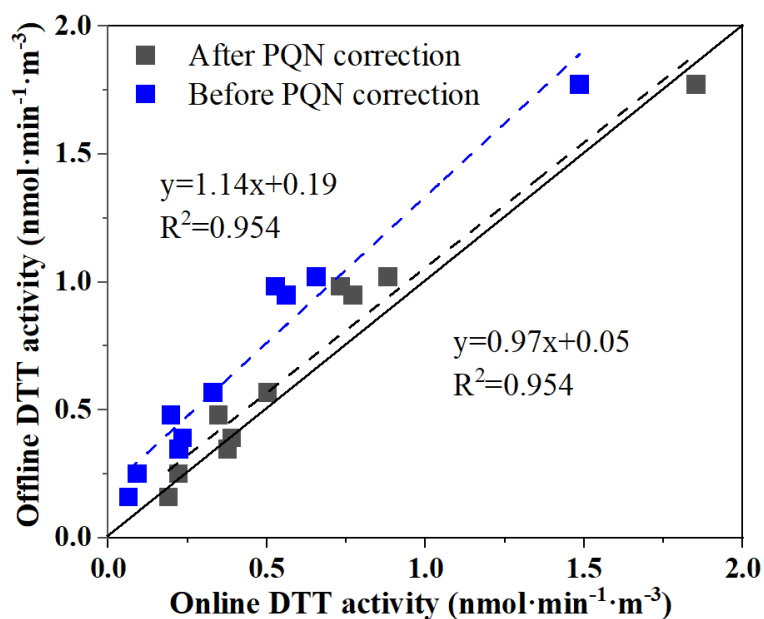
578

Figure 4. Blank corrected DTT consumption rate as a function of PQN used as a positive control. Each error bar represents the standard deviation of three independent DTT measurements on each concentration.



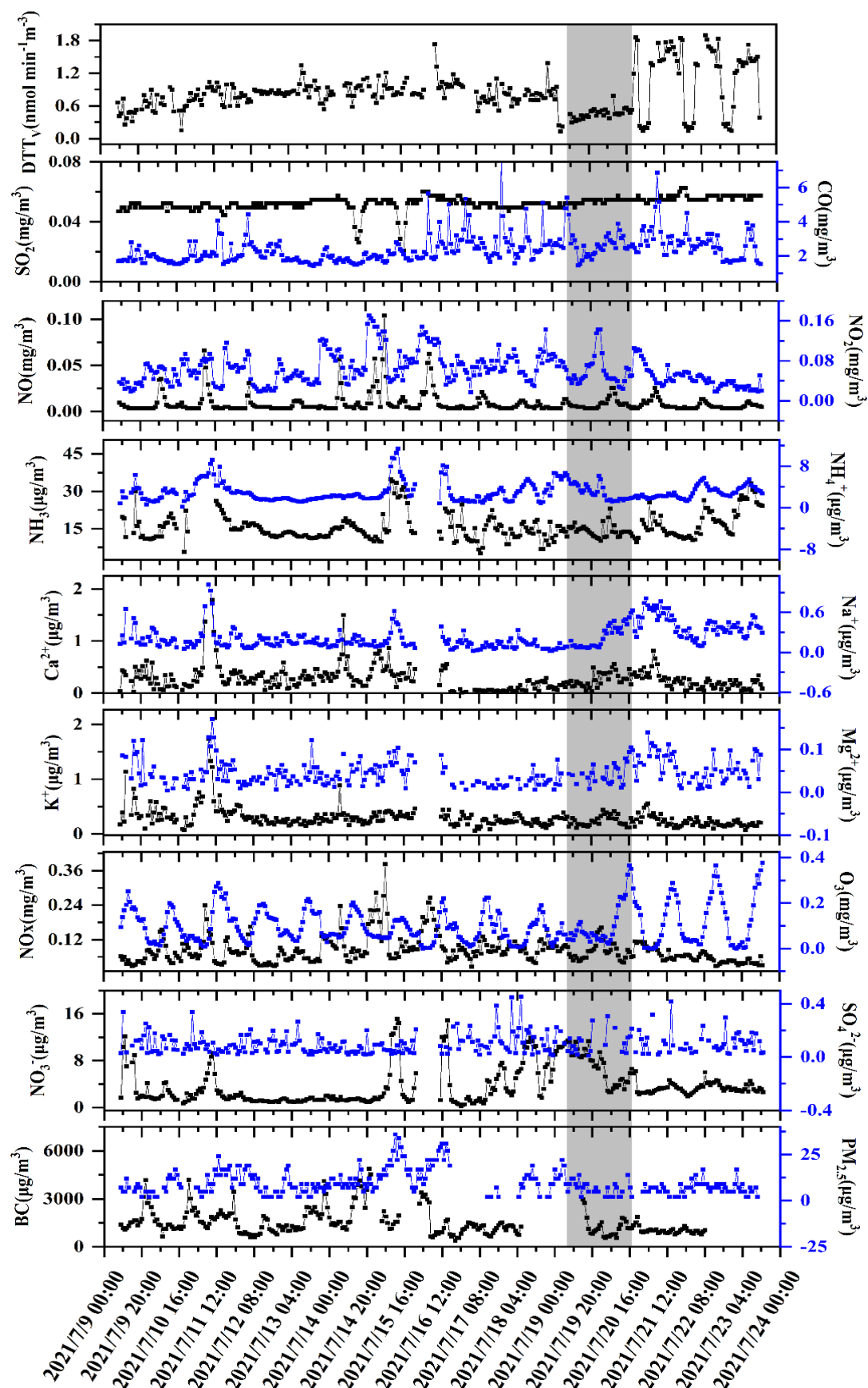
579

580 **Figure 5.** Comparison of the automated system with manual operation using PQN (9,10-
 581 phenanthraquinone)



582

583 **Figure 6.** Comparison of the automated system with manual operation using ambient aerosol
 584 extracts (PM_{2.5} samples collected from Xuzhou, regression analysis is done by orthogonal
 585 regression; the line is 1:1).
 586



587

588

Figure 7 . Time series of the DTT activity, PM_{2.5} water-soluble components (SO₄²⁻, NO₃⁻, NH₄⁺, Na⁺, Ca²⁺, K⁺) and polluting gases (SO₂, CO, O₃, NH₃) (The shaded part is rainy weather)

589

590

591 **Table 1.** The correlation coefficient (R) between the concentration of water-soluble chemical
 592 substances in environmental PM_{2.5} (µg m⁻³) and the volume normalized substance concentration
 593 (DTTV), before rain, during rain, and after rain.

Parameter	Total	Before it rains	During rain	After rain
PM _{2.5}	0.014	0.305**	0.026	-0.290*
SO ₂	0.195**	0.114	-0.136	0.222
NO	-0.029	-0.029	-0.074	0.050
NO ₂	-0.098	0.115	0.169	-0.203
NO _x	-0.085	0.062	0.142	-0.169
CO	-0.033	0.146*	-0.093	0.121
O ₃	0.227*	0.153	0.044	0.624**
BC	-0.052	-0.054	-0.439*	0.087
NH ₃	0.241**	0.074	-0.129	0.269*
SO ₄ ²⁻	-0.06	-0.065	0.329	0.028
NO ₃ ⁻	-0.163*	-0.155*	-0.352*	0.511**
NH ₄ ⁺	0.024	0.028	0.062	0.271*
K ⁺	-0.077	-0.045	0.125	-0.337**
Mg ²⁺	0.131*	0.075	0.233	0.086
Ca ²⁺	0.005	0.072	0.021	-0.055
Na ⁺	0.177**	-0.007	0.133	0.008

594

PM_{2.5}, particulate matter with an aerodynamic diameter < 2.5µm; *P<0.05, **P<0.01.

595